EFFECT OF SLOSHING ON SHIP MOTIONS

Olav F. Rognebakke and Odd M. Faltinsen
Department of Marine Hydrodynamics
Norwegian University of Science and Technology
N-7491 Trondheim, Norway

When a ship carrying liquid cargo moves in waves, sloshing may occur. The ship motions excite sloshing which in return affects the ship motions. 2-D experiments on a box-shaped ship section excited by regular beam sea have been conducted to study this coupling effect. The section contains two tanks and can only move in sway. The external ship motion problem may be solved by using a standard linear strip theory program, while the sloshing must be described by a nonlinear method. The adaptive multimodal approach by Faltinsen and Timokha [1] has been used. This method has been extensively validated for forced tank motions. The present study represents a first validation for coupled internal and external flows.

The experiments were carried out in the wave flume of the Department of Marine Hydrodynamics at NTNU. The flume has an overall length of 13.5 m and is 0.6 m wide. It is equipped with an electronically operated, computer controlled, single flap wavemaker, calibrated for a water depth of 1.03 m. The side walls and the bottom of the flume are made of glass.

Fig. 1 shows model parameters. The ship section with an overall length of 596 mm has 2 mm clearance from the flume walls. The breadth is 400 mm and the draft 200 mm. The two identical tanks have breadth b of 376 mm, a length of 150 mm and a height of 288 or 388 mm depending on the position of the deck. The deck may be lowered when sloshing induced water impact on the tank roof is desirable. No tank roof impact occurred in the reported examples. Weights are added to the model so that the total weight equals the buoyancy for the fixed draft and different amounts of water in the tanks. The section slides along two rails where low friction bearings are used. It is restrained from drifting off by springs with a total stiffness of 30.9 N/m. The springs cause an eigenfrequency well below the studied wave frequencies. The steepness of the waves was kept below a certain threshold value to prevent breaking. Fig. 2 gives the chosen relation between frequency ω and amplitude ζ_a of the generated regular waves.

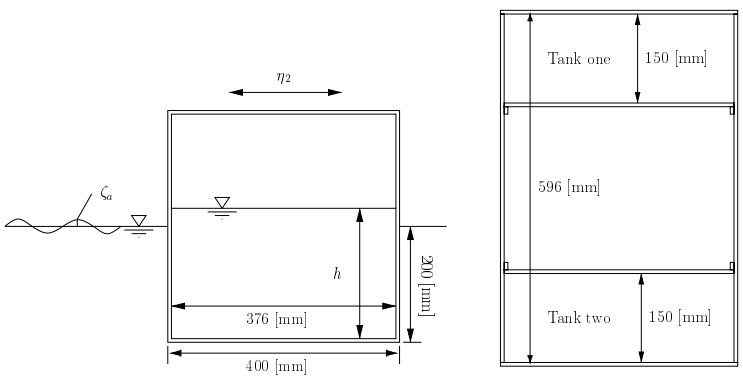

Figure 1: Box-shaped ship section, side and top view

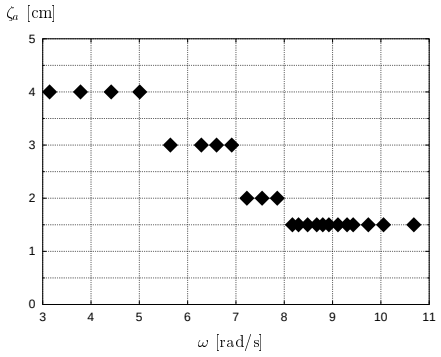

Figure 2: Relationship between wave amplitude and wave frequency

A typical time series for the sway motion of the section with water in one tank, is shown in Fig. 3. A transient phase precedes a steady state for the system. A beating period of ≈ 5 s is evident during the transient phase. This is the eigenperiod of the system consisting of the springs and the ship model. A shift in mean position of the section occurs due to 2nd order drift force. The steady state motions show almost no higher order harmonics. This indicates that the higher order part of the sloshing force is filtered out by the system. The steady state phase is short for long waves and consequently the uncertainties in measured sway amplitude increase. For wave periods very close to the first natural period of the fluid in the tanks an unstable situation may occur. The sway amplitude shifts and thus two steady state responses take place during one run. In the experimental data presented later where one tank is filled with $h = 0.184$ m, this can be seen as two very different measured sway amplitudes for a wave frequency $\omega = 8.65$ rad/s. This is associated with jumps between different branches of the steady-state sloshing solution [2]. The steady state ends when waves reflected from the wavemaker and the beach reach the model.

Measured and calculated sway amplitudes for empty tanks have been compared to validate the accuracy of the measurements, (see Fig. 4). A standard linear seakeeping program was used in the calculations. The

experimental results for rigid mass agree well with the computed values.

Fig. 4 illustrates the large effect of the fluid motion inside the tanks. When ω is smaller or slightly higher than the lowest linear eigenfrequency σ_n of the fluid motion in the tanks, a sway response lower than for a rigid fluid mass is observed for half-filled tanks. The force resulting from the fluid motion in the tanks acts against the sway excitation force in this case. When $\omega \approx \sigma_n$ the sway motion is almost zero. For ω slightly above σ_n the sway motion increases due to the fluid in the tanks. This behaviour can be qualitatively explained by using a linear model for the sloshing. The phase of the sloshing force shifts 180° when the excitation frequency moves from below to above the first natural frequency.

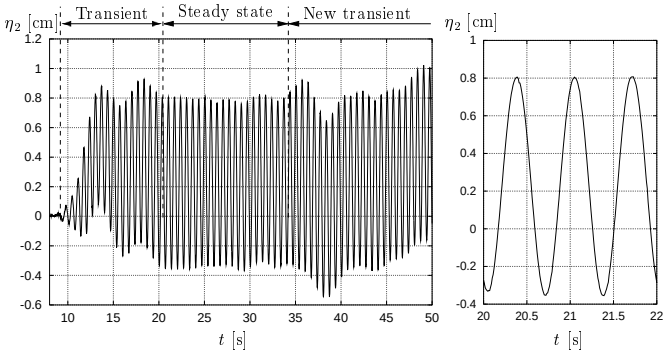

Figure 3: Example of time history of the sway motion of the ship section. $\omega = 9.42$ rad/s and $\zeta_a = 0.015$m

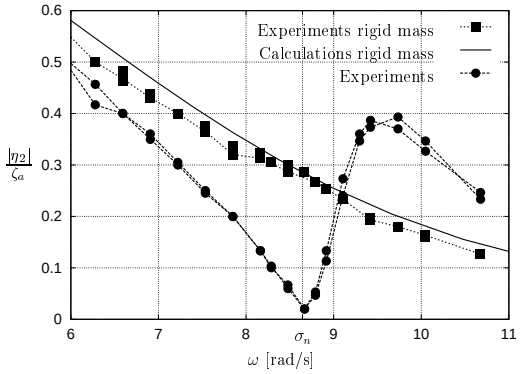

Figure 4: Sway amplitude for rigid mass and for two tanks filled with $h = 0.184$ m

The change with wave frequency of the phasing between the forces acting on the model is visually apparent from Fig. 5. The right plot in this figure gives the experimental values for sway motion when one of the tanks is filled with $h = 0.184$ m. Snapshots show the instantaneous position of the free surface both inside the tank and outside the ship section, for three different wave frequencies. The phasing between the internal and external fluid motion permits to qualitatively understand why the internal fluid motion can either amplify or reduce the ship motion. The phasing is evident from the relative vertical motion of the free surfaces inside and outside the model.

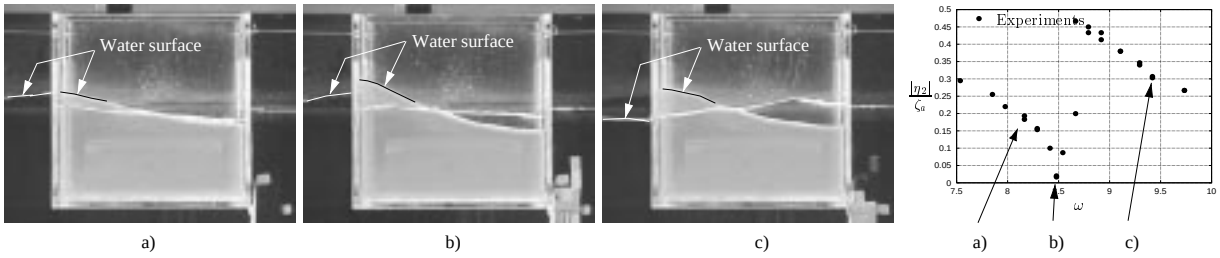

Figure 5: Motion of fluid inside and outside the tank. $h = 0.184$ m. One tank is filled

An interesting phenomenon is observed for wave frequencies close to the resonance for the fluid motion in the tanks. When the wave front hits the model, a significant sway motion is initiated. This in turn excites sloshing in the tanks, and thus a sloshing force starts to counteract the excitation force from the waves. The sway motion decreases until an equilibrium is reached. At this stage the sway induced sloshing force almost balances the excitation force from the waves. However, since $\omega \approx \sigma_n$ a very small sway motion causes a violent sloshing response.

Fig. 6 shows experimental and computed values of the sway motion of the model for different filling levels of one or two tanks. The first linear eigenfrequency σ_n is indicated in the plots. Calculated values found by using an analytical linear and nonlinear sloshing solution and a standard linear seakeeping program for the external flow are presented for all cases. The calculations based on the linear sloshing model follow the general trend of the experiments. However, the sway amplitude is consistently over-predicted for frequencies right above σ_n. The reason is that the linear sloshing force is either in phase or exactly 180° out of phase with the position of the model. Actually, the phase transition occurs over a certain range of frequencies. Furthermore, when a large percentage of the sloshing force acts in phase with the mass and added mass forces and works against them, the increased motion results in an increased sloshing force amplitude. When the frequency is equal to σ_n

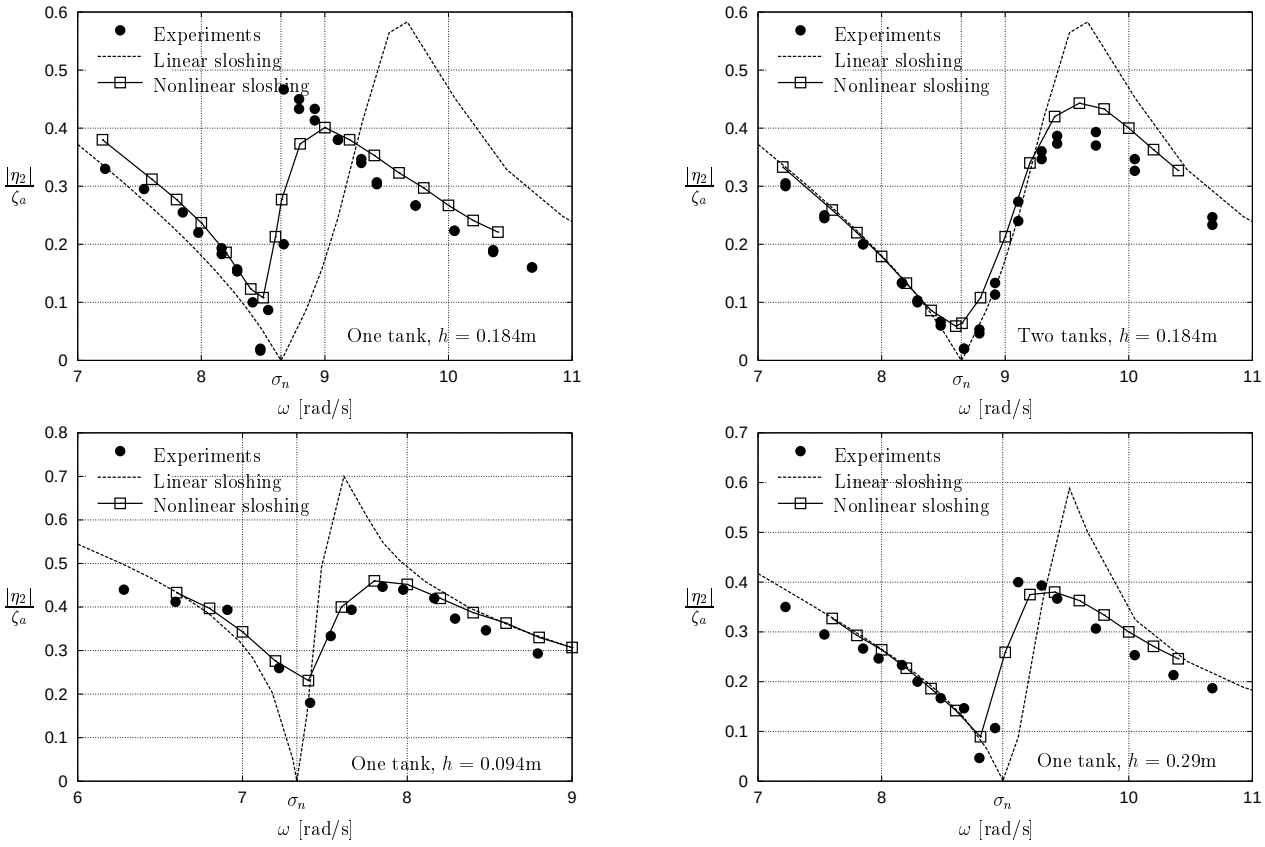

Figure 6: Comparisons between experiments and calculations

in the linear sloshing model the resulting sloshing force is infinite for finite sway motion. The combination of the linear sloshing force with the dynamics of the model cause zero sway for $\omega = \sigma_n$, while in reality the sway motion will have a minimum different from zero in the vicinity of σ_n.

The linear sloshing model fails in predicting the frequency of minimum sway motion for the three cases when only one tank is filled, since the large amplitude sloshing at resonance invalidates the assumption of a constant natural frequency for the internal fluid motion. In [2] it is shown how the first natural frequency varies as a function of the sloshing amplitude. When the filling height h is below the critical value $h/b = 0.3374$, σ_n increases as the amplitude increases. This explains the discrepancy in minimum sway by the linear sloshing model for $h = 0.094$ m. For $h = 0.29$ m and 0.184 m, the water level is above the critical depth and consequently the experiments show a minimum below σ_n. When $h = 0.184$ m and two tanks are filled, the amplitude of the sloshing motion at $\omega \approx \sigma_n$ is rather small. Hence the linear sloshing model gives an acceptable result.

In the computational results where the nonlinear model is included, the equation of motion Eq. (1) is solved in time and coupled with the nonlinear sloshing model.

$$(M + A_{22})\,\ddot{\eta}_2 + B_{22}\dot{\eta}_2 + C_{22}\eta_2 - F_{\text{exc}}(\zeta_a) - F_{\text{slosh}}(\eta_2) = 0 \tag{1}$$

In (1) M is structural mass excluding internal fluid mass, A_{22} and B_{22} are the frequency dependent added mass and damping due to the external linear flow, C_{22} is the linear spring coefficient, F_{exc} is the horizontal linear wave excitation force and F_{slosh} is the horizontal force caused by sloshing. The simulations are prolonged until steady state sway motion is achieved. The external flow model needs justification. A proper linear external model should be based on the methodology presented by Cummins [3] which implies that the radiation force is a function of convolution integrals. This would be needed in order to calculate the transient phase of the external flow and sloshing induced higher order harmonic motions. But several authors, e.g. Adegeest [4], report difficulties in applying such a formulation in practice. Actually the influence of higher harmonics in the sloshing force is negligible. This can be seen from spectral analysis of the sway motion time history. In our case, since we focus on the steady-state motions, the present external force model represents a satisfactory approximation.

By including a nonlinear sloshing model a better agreement between the calculations and the experiments is obtained. For instance a much improved prediction of the minimum sway motion is achieved.

The computed sway amplitudes for two tanks and $h = 0.184$ m were found to be sensitive to the level of damping chosen for the sloshing motion. Fig. 7 shows how the damping of the internal flow affects the results

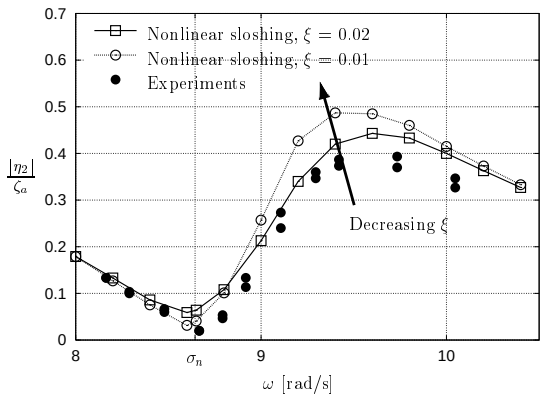

Figure 7: Experimental and computed sway amplitudes for two tanks, $h = 0.184$ m. Effect of sloshing damping ξ

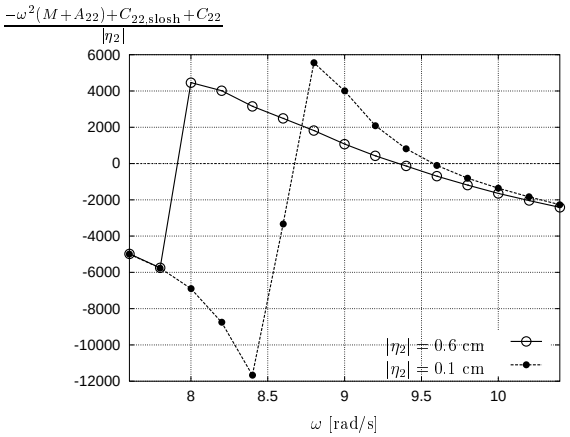

Figure 8: Mass terms - in phase with sway acceleration $\ddot{\eta}_2$

when a variation from 2% to 1% of the critical damping is considered. A description of how damping is included in the sloshing model can be found in [2]. This damping may represent e.g. viscous effects or local breaking and is not rationally predicted. The effect of external vortex shedding at the sharp corners was studied and found to be small. For $\omega > \approx \sigma_n$ the sway amplitudes increase with a decreasing damping, while around sloshing resonance the motion becomes smaller. In order to explain this phenomenon, the balance between the different terms in the equation of motion was studied. A quasi-linear approach was applied. The sum of the terms in or 180° out of phase with the sway accelerations are presented in Fig. 8. The contribution from the sloshing force is expressed as a frequency dependent restoring term $C_{22,\text{slosh}}$. By making an analogy with a linear system the zero of this sum corresponds to an eigenfrequency for the sway motion. The sum is close to zero just above or below $\omega = 9.5$ rad/s for the two amplitudes of steady state sway motion presented. Further, the sloshing force is large and nearly 180° out of phase with the acceleration in the vicinity of this frequency. Thus a small change in the phasing will lead to an important alteration of the part of the sloshing force which can be considered as a damping term for the coupled system. The damping terms are in this case all that balances the external force. For the example presented in Fig. 7 a phase change of 5° for F_{slosh} at $\omega = 9.4$ rad/s leads to a change of 10% in the sway motion. The phase is a function of the damping of the fluid motion inside the tanks. This explains the observed theoretical behaviour. If heavy tank roof impact had occurred, the damping of the internal fluid motion would be dominated by tank roof impact damping, [5]. Since the latter damping component can be rationally calculated, the ambiguity in selecting ξ demonstrated in Fig. 7 would be unimportant.

Further work will include the effect of tank roof impact. A natural next step is to include the roll and heave motion in the 2-D model before starting on a 3-D analysis to avoid that too many physical effects are included simultaneously in a complicated dynamic system.

Acknowledgements

This work is part of a Ph. D. thesis sponsored by the Research Council of Norway.

References

[1] Faltinsen, O. M. and Timokha, A. N. (2001) Adaptive multimodal approach to nonlinear sloshing in a rectangular tank., *J. Fluid Mech.*

[2] Faltinsen, O. M., Rognebakke, O. F., Lukovsky, I. A., Timokha, A. N. (2000) Multidimensional modal analysis of nonlinear sloshing in a rectangular tank with finite water depth., *J. Fluid Mech.*. **407**, 201-234

[3] Cummins, W. E. (1962), The impulse-response function and ship motions. *Schiffstechnik 9*(47), 101-109

[4] Adegeest, L. J. M. (1995), Nonlinear hull girder loads, Ph.D. thesis, Delft University of Technology, Faculty of Mechanical Engineering and Marine Technology

[5] Rognebakke, O. F. and Faltinsen, O. M (2000), Damping of sloshing due to tank roof impact, *15th International Workshop on Water Waves and Floating Bodies*, Caesarea, Israel